UPPSALA
UNIVERSITET

MASTER THESIS

Quantum Landau-Lifshitz-Gilbert Dynamics of a Dimer

Student:
Lee Johnson
lee.johnson.6294@student.uu.se

Supervisor:
Erik Sjöqvist
erik.sjoqvist@physics.uu.se

Department of Physics and Astronomy

October 11, 2022

Abstract

The classical Landau-Lifshitz-Gilbert (LLG) equations are of crucial importance in micro-magnetism, but a true quantum-mechanical description was not found until 2013. However, very few realistic quantum systems have been modeled using it.

This project describes the quantum LLG dynamics of a dimer system, accounting for the Heisenberg exchange and Dzyaloshinskii-Moriya interactions, as well as local dephasing as an open system effect. Equations of motion are derived using an appropriate Hamiltonian, Wieser's non-linear master equation and a two-qubit parametrization, then solved numerically. The non-locality and entanglenment of the system were then investigated using the CHSH inequality and concurrence.

The solutions for the dimer system show oscillations in the Bloch vector components aligned with the external magnetic field, and in the anti-ferromagnetic case, both CHSH inequality violation and entanglement were initially found, but underwent "sudden death" and disentanglement as the evolution continued, due to dephasing. Analysis of the kT-B_z parameter space reveals combinations which produce entanglement without violation of the Clauser, Horne, Shimony, Holt (CHSH) inequality, and regions of B_z where increasing kT increases entanglement.

This set of solutions to Wieser's quantum LLG equation suggests that the disentangling effect of dephasing and other open-system effects will be obstacles for future practical efforts in quantum communication.

Forskare löser en ny kvantlik Landau-Lifshitz-Gilbert-ekvation

Landau-Lifshitz-Gilbert-ekvationen används inom flertal vetenskapliga fält. Även om den beskriver de magnetiska momenten hos partiklar i ett material används den långt utanför tillämpad magnetism, på så olika områden som datalagring, medicin och kemi. Men ekvationen tog inte hänsyn till kvantmekaniken förrän 2013, då Wieser tog fram en kvantversion av ekvationen. Hittills har ekvationen dock bara lösts för de mest grundläggande situationerna. I denna rapport har dess beteenden undersökts för en mer realistisk modell, och i processen har avslöjats problem för framtida ansträngningar inom kvantkommunikation och datalagring.

Forskningen innebar att man löste Wiesers ekvation för ett ”dimer”-system, det vill säga ett system som består av två kvantbitar. I termer av kvantinformation är en kvantbit något som kan anta två värden, på samma sätt som en bit i en dator kan vara 0 eller 1. Detta gäller för spinnet hos en elektron, och det är precis vad Wiesers ekvation kan användas för att modellera. Själv löste han den bara för ett spinn, vilket innebär att arbetet ignorerade interaktionerna mellan elektroner som kan spela en viktig roll för hur de beter sig.

Lösningarna till Wiesers ekvation för ferromagnetiska och antiferromagnetiska dimerer visade på vissa förväntade beteenden. För det första anpassar sig partiklarnas spinn till varandra i det ferromagnetiska men inte i det antiferromagnetiska fallet, och storleken på spinnvektorerna minskar under tidsutvecklingen. Dessutom fanns det ett karakteristiskt kvantmässigt ”ickelokalt” beteende i det anti-ferromagnetiska men inte i det ferromagnetiska fallet.

Sammanflätning kan beskrivas som en korrelation mellan två partiklar, som är så stark att man inte kan beskriva den ena partikelns tillstånd utan att hänvisa till den andra. Detta har visat sig vara en värdefull resurs för kvantkommunikation, vilket möjliggör tillämpningar som tät kodning och kvantteleportering, samt används i många kvantkryptografiska system. Detta erhölls när ekvationen löstes för en anti-ferromagnetisk dimer, men det fanns en hake. Eftersom forskarna införlivade ”öppna systemeffekter” - det vill säga dimersystemets interaktion med den omgivande miljön - försvann snart sammanflätningen i många fall.

Denna ”finita tidsupplösning” och den därmed sammanhängande ”plötsliga döden av icke-lokalitet” avslöjade ett problem för praktisk kvantkommunikation. Närvaron av effekterna av öppna system, som kommer att vara mycket svåra att undvika i alla verkliga system, förstör den kvantkorrelation som man hoppas kunna utnyttja i kvantkommunikationen. De nya lösningarna ger en bättre inblick i Wiesers ekvation, men avslöjar också ett allvarligt problem som fysiker och ingenjörer måste ta itu med om kvantkommunikation någonsin ska kunna användas i praktiken.

Contents

1 Introduction

The Landau-Lifshitz-Gilbert (LLG) equation is essential to the study of dynamical systems in applied magnetism [1], and has a huge range of applications in fields ranging from chemistry [2] and medicine [3] to astronomy [4] and data storage [5]. The atomistic version of the LLG equation forms the basis for the description of atomistic spin dynamics. It involves the magnetic moments $\mathbf{m}_k$ at crystal sites k, and takes the form:

$$\dot{\mathbf{m}}_k = -\gamma \mathbf{m}_k \times \mathbf{B}_k + \mathbf{m}_k \times \sum_l \alpha_{kl} \frac{1}{|\mathbf{m}_l|} \dot{\mathbf{m}}_l, \tag{1}$$

where γ is the gyromagnetic ratio and α_{kl} is the non-local damping rate.

While this atomistic form can be derived from first principles [6], prior to the work by Wieser [7], the LLG equation itself was a purely phenomenological result that described the classical motion of a magnetic moment under the influence of a magnetic field. In reality, the apparent motion of the magnetic moment actually stems from the underlying quantum motion of the spin state of the constituent particles.

Wieser [7] addressed this shortcoming by deriving an equivalent quantum equation from the starting point of the time-evolution of a quantum state. He used a non-Hermitian Hamiltonian to model the dissipative effect from the Gilbert term (the second term in Eq. (1)). This resulted in the non-linear master equation:

$$\dot{\rho} = i[\rho, H] - \lambda[\rho, [\rho, H]], \tag{2}$$

where ρ is the density operator for the system, and H is its Hamiltonian. We propose that this can be considered the lowest-order form of the new, more general equation:

$$\dot{\rho} = i[\rho, H] + i\lambda[\rho, \dot{\rho}], \tag{3}$$

where Eq. (2) is recovered from Eq. (3) by simply putting its first term in

place of the $\dot{\rho}$ in the commutator.

This represents a step forwards in describing the quantum mechanical reality behind the phenomenological behaviour, and it generated much interest as an avenue to study the quantum-classical transition [8, 9]. However, Wieser's analysis [7] has some limitations. Firstly, it only addresses the local version of the LLG equations, where $\alpha_{kl} \propto \delta_{kl}$, and secondly, it did not account for spin-spin interactions and other effects which make up a genuinely quantum-mechanical description of the system.

This work aims to address these shortcomings by considering the evolution of the spin states of a (two-qubit) dimer, accounting for the Heisenberg exchange interaction [10] and the Dzyaloshinskii-Moriya (DM) interaction [11]. In addition, dephasing is one of the main obstacles for the production and operation of quantum information devices [12]. This is caused by the continuous interaction of the system with its environment [13], which results in states losing their purity over time. Therefore, any analysis of the quantum dynamics of a dimer should account for these factors if it is to be applicable to real-world systems.

Two-particle quantum systems such as this can also display the excess quantum correlations known as entanglement, and this was identified by Wieser [8] as one of the major reasons multi-spin systems exhibit non-classical behaviour. Entanglement was described by Schrödinger [14] as *"the* characteristic trait of quantum mechanics, the one that enforces its entire departure from classical lines of thought." For pure systems, a pair is entangled if they cannot be factorised into separate pure states, with the singlet state of two spin-1/2 particles being a common example:

$$|\psi\rangle = \frac{1}{\sqrt{2}}(|\uparrow\downarrow\rangle - |\downarrow\uparrow\rangle).$$

In this state, neither particle has a clearly defined state, and yet, even if separated by a large distance, they will remain perfectly anti-correlated to each other: if particle one is detected in the spin-up state, particle two will be detected in the spin-down state and vice-versa.

The famous 1935 Einstein-Podolsky-Rosen (EPR) paper [15] suggested that local, hidden-variable theories could explain these excessive correlations, through an example often called the "EPR paradox." However, Bell [16] and later, Clauser *et. al.* [17] found that there is a limit to the amount of correlation that can be explained by local hidden variable theories, and quantum mechanics predicts a violation of these inequalities. While Bell also derived them in a different form, the Clauser, Horne, Shimony and Holt (CHSH) form of the inequalities remain a widely-used measure of non-locality.

Since the EPR paper and Bell's solution to the apparent paradox, entanglement has been increasingly identified as a crucial resource in quantum information processing [18], allowing uniquely quantum feats such as teleportation and dense coding [19]. It is on this basis that efforts to quantify and measure entanglement have gained steam, resulting in measures like the relative entropy of entanglement [20]. This is equal to the von Neumann entropy of the reduced density matrix of one qubit from the pair.

There are many other potential measures for entanglement, but one particularly useful approach is concurrence [19]. This comes from work defining the entanglement of formation, and will be defined in more detail in Section 6. Simply put, it allows a precise, information-based and practical approach to quantifying entanglement.

With this all in mind, this work intends to derive equations of motion for a dimer system using the non-linear master equation (Eq. (2)), solve for its Bloch vectors and correlation matrix, and then go on to analyze non-locality and entanglement in the system, through the CHSH inequality [17] and concurrence [19].

2 Setting Up the Model

Wieser's [7] non-linear master equation, Eq. (2), will be used, with the Lindblad term added to account for open system effects:

$$\dot{\rho} = i[\rho, H] - \lambda[\rho, [\rho, H]] + L(\rho), \tag{4}$$

where $L(\rho)$ is the Lindblad term. The three key elements of this will be discussed in this section.

2.1 Spin-Spin Interaction Hamiltonian

The model considered is described by the Hamiltonian:

$$H = \vec{B}(\vec{\sigma}_1 \otimes \hat{1} + \hat{1} \otimes \vec{\sigma}_2) + J\vec{\sigma}_1 \cdot \otimes\vec{\sigma}_2 + \vec{D} \cdot \vec{\sigma}_1 \times \otimes\vec{\sigma}_2, \tag{5}$$

where $\vec{\sigma}$ are vector versions of the Pauli matrices (i.e. $\vec{\sigma} = \{\sigma_x, \sigma_y, \sigma_z\}$), J is the coupling constant for the Heisenberg exchange interaction, $\vec{D}$ is the DM-interaction vector and $\vec{B}$ is the magnetic field vector. The subscripts 1 and 2 refer to the individual qubits. We will take $\hbar = 1$ throughout.

The first term is the Zeeman term, the second is a Heisenberg exchange term, with $J > 0$ for an antiferromagnetic dimer and $J < 0$ for a ferromagnetic dimer, and the third is a DM term. The latter two are two of the most important spin-spin interactions, but additional interactions could be easily incorporated.

For simplicity, we shall assume that the magnetic field is entirely in the z-direction and the DM vector is also aligned in this direction. The explicit form of the Hamiltonian in this case is therefore:

$$\begin{aligned} H =& B_z(\sigma_{1,z} \otimes \hat{1} + \hat{1} \otimes \sigma_{2,z}) + J(\vec{\sigma}_1 \cdot \otimes\vec{\sigma}_2) \\ &+ D_z(\sigma_{1,x} \otimes \sigma_{2,y} - \sigma_{1,y} \otimes \sigma_{2,x}). \end{aligned} \tag{6}$$

Note that there is no loss of generality in taking the magnetic field to be aligned in the z-direction: any other orientation can be obtained with an appropriate rotation of coordinate system. However, some generality will be

lost in taking the DM-interaction to be aligned in the same way. This choice is for simplicity.

2.2 Two Qubit Bloch Vector Parametrization

For the Hilbert space $\mathcal{H} = C^2 \otimes C^2$, we can use the Hilbert-Schmidt basis to represent the dimer state [21, 22]. This results in the following unit trace density matrix:

$$\varrho = \frac{1}{4}(\hat{1} \otimes \hat{1} + \vec{r} \cdot \vec{\sigma}_1 \otimes \hat{1} + \hat{1} \otimes \vec{s} \cdot \vec{\sigma}_2 + T_{kl}\sigma_{1,k} \otimes \sigma_{2,l}), \tag{7}$$

where T_{kl} are the components of the correlation matrix and the $\sigma_{1,k}$ and $\sigma_{2,l}$ are the corresponding Pauli matrices. The $\vec{r}$ and $\vec{s}$ terms are the marginal Bloch vectors for each qubit, which describe the states as positions on the unit radius Bloch ball.

2.3 Open System Effects: Dephasing

The Lindblad term in Eq. (4) can be expressed as:

$$L(\rho) = \sum_k (L_k \rho L_k^\dagger - \frac{1}{2} L_k^\dagger L_k \rho - \frac{1}{2} \rho L_k^\dagger L_k), \tag{8}$$

where the L_k are Lindblad operators [23]. This model only considers the effect of local dephasing, so the operators take the form:

$$\begin{aligned} L_1 &= \sqrt{\gamma}\sigma_{1,i} \otimes \hat{1}, \\ L_2 &= \sqrt{\gamma}\hat{1} \otimes \sigma_{2,i}, \end{aligned} \tag{9}$$

where the i stands in for the direction the interaction is considered in. For this project, dephasing will be considered in the z direction. This reduces generality, because the dephasing is aligned with the external field, but simplifies the present analysis. It is important to note that this formalism assumes Markovian dynamics, so that during each small time step, the system undergoes a completely positive trace preserving transformation. In essence, this assumes that the environment does not memorize its interaction with the system.

3 Deriving Equations of Motion

Given the assumptions and setup above, the two-qubit parametrization, Hamiltonian and Lindblad terms can be combined for use in the non-linear master equation, Eq. (4).

3.1 Useful Formulae

There are a number of formulae that were used through the derivation. Most importantly, the Pauli matrices:

$$\sigma_x = \begin{pmatrix} 0 & 1 \\ 1 & 0 \end{pmatrix}, \ \sigma_y = \begin{pmatrix} 0 & -i \\ i & 0 \end{pmatrix}, \ \sigma_z = \begin{pmatrix} 1 & 0 \\ 0 & -1 \end{pmatrix}, \tag{10}$$

have the commutation relations:

$$[\sigma_i, \sigma_j] = 2i\epsilon_{ijk}\sigma_k, \tag{11}$$

where ϵ_{ijk} is the Levi-Civita symbol. Products are also formed as follows:

$$\sigma_i\sigma_j = \delta_{ij}\hat{1} + i\epsilon_{ijk}\sigma_k, \tag{12}$$

where δ_{ij} is the kronecker delta, and the Einstein summation convention is used so that repeated indices are summed. Tensor products also obey the following:

$$(A \otimes B)(C \otimes D) = AC \otimes BD. \tag{13}$$

We take the same approach as other authors [24], using the extended Pauli matrices (with $\sigma_0 = \hat{1}$, the identity matrix) and make Dirac matrices, which take the form:

$$D_{\mu\nu} = \sigma_\mu \otimes \sigma_\nu. \tag{14}$$

Note that we have $i, j, k, ... \in 1, 2, 3$ and $\alpha, \beta, \gamma, ... \in 0, 1, 2, 3$.

Using Eqs. (12), (13) and (14), it can be established that:

$$\begin{aligned} D_{\alpha\beta}D_{\gamma\delta} &= (\theta_{\alpha\gamma\mu} + i\epsilon_{\alpha\gamma\mu})(\theta_{\beta\delta\nu} + i\epsilon_{\beta\delta\nu})D_{\mu\nu} \\ [D_{\alpha\beta}, D_{\gamma\delta}] &= 2i(\theta_{\alpha\gamma\mu}\epsilon_{\beta\delta\nu} + \epsilon_{\alpha\gamma\mu}\theta_{\beta\delta\nu})D_{\mu\nu}, \end{aligned} \tag{15}$$

where $\epsilon_{\alpha\beta\gamma}$ is again the Levi-Civita tensor and the $\theta_{\alpha\beta\gamma}$ tensors are defined:

$$\theta_{\alpha\beta\gamma} = \begin{cases} 1, \text{ when one index is 0 and the others are equal,} \\ 0, \text{ otherwise.} \end{cases} \tag{16}$$

3.2 Derivation

While the full details of the derivation of the formulae are lengthy (see Appendix), the overall strategy was very straightforward. The two-qubit parametrization, Hamiltonian and Lindblad terms were inserted into Eq. (4) and the commutators calculated with *Mathematica*. Most of this was accomplished with the formula in Eq. (17).

This process led to a long expression that can be arranged in coefficients of the Dirac matrices. For example:

$$\begin{aligned} \dot{\rho} = ...+2iD_{0x}\Bigg(&\frac{1}{2}(-B_z s_y + DT_{xz} + JT_{yz} - JT_{zy}) + \frac{1}{4}L\big((-Jr_x + Js_x + Ds_y - B_z T_{xz})T_{yy} \\ &- T_{xz}(-Jr_z + Js_z - B_z T_{xx} + B_z T_{yy}) + s_y(DT_{xx} - JT_{xy} + JT_{yx} + DT_{yy}) \\ &- (Dr_z - Ds_z - B_z T_{xy} - B_z T_{yx})T_{yz} + T_{xy}(Jr_y + Ds_x - Js_y + B_z T_{yz}) \\ &- s_z(-B_z s_x + JT_{xz} - DT_{yz} - JT_{zx}) - (Jr_x - Dr_y - Js_x - B_z T_{zx})T_{zz}\big)\Bigg) + ... \end{aligned}$$

This shows the part of the right hand side which is a coefficient of D_{0x}, which is then matched with the corresponding coefficient on the left hand side. In this way, 15 equations were derived, for three components each for the two Bloch vectors and the nine entries of the correlation matrix T_{kl}. The Dirac matrix basis would lead to 16 equations in this way, but the D_{00} term is accounted for by the fixed $\frac{1}{4}\hat{1}\otimes\hat{1}$ term in the two-qubit parametrization (Eq. (7)).

3.3 Equations of Motion

The equations of motion were derived in full using Eq. (4) (see Appendix A). This is Wieser's master equation, for two spins, plus Lindblad terms. However, using the more general non-linear master equation, Eq. (3), along with Lindblad terms allows a much neater form to be found. This is not the version solved for this analysis, but will likely produce very similar results, especially with a low value for the non-linear parameter λ:

$$\begin{aligned}
\dot{r}_x &= 2(-r_y B_z + T_{yz}J - T_{zy}J + T_{zx}D - \gamma r_x) - \frac{\lambda}{2}(\dot{r}_y r_z - \dot{r}_z r_y + \dot{T}_{yx}T_{zx} \\
&\quad + \dot{T}_{yy}T_{zy} - \dot{T}_{zx}T_{yx} - \dot{T}_{zz}T_{yz} + \dot{T}_{yz}T_{zz} - \dot{T}_{zy}T_{yy}) \\
\dot{r}_y &= 2(B_z r_x - T_{xz}J - T_{zx}J + T_{zy}D - \gamma r_y) - \frac{\lambda}{2}(-\dot{r}_x r_z + \dot{r}_z r_x - \dot{T}_{xx}T_{zx} \\
&\quad - \dot{T}_{xz}T_{zz} + \dot{T}_{zx}T_{xx} - \dot{T}_{xy}T_{zy} + \dot{T}_{zz}T_{xz} + \dot{T}_{zy}T_{xy}) \\
\dot{r}_z &= 2(-T_{xx}D + T_{xy}J + T_{yx}J - T_{yy}D) - \frac{\lambda}{2}(\dot{r}_x r_y - \dot{r}_y r_x + \dot{T}_{xx}T_{yx} + \dot{T}_{xy}T_{yy} \\
&\quad - \dot{T}_{yx}T_{xx} - \dot{T}_{yy}T_{xy} + \dot{T}_{xz}T_{yz} - \dot{T}_{yz}T_{xz}) \\
\dot{s}_x &= 2(-s_y B_z - T_{xz}D - T_{yz}J - T_{zy}J - \gamma s_x) - \frac{\lambda}{2}(\dot{s}_y s_z - \dot{s}_z s_y + \dot{T}_{xy}T_{xz} + \\
&\quad \dot{T}_{yy}T_{yz} - \dot{T}_{xz}T_{xy} - \dot{T}_{zz}T_{zy} - \dot{T}_{yz}T_{yy} + \dot{T}_{zy}T_{zz}) \\
\dot{s}_y &= 2(s_x B_z + T_{xz}J - T_{yz}D - T_{zx}J - \gamma s_y) - \frac{\lambda}{2}(-\dot{s}_x s_z + \dot{s}_z s_x - \dot{T}_{xx}T_{xz} - \\
&\quad \dot{T}_{yx}T_{yz} + \dot{T}_{xz}T_{xx} - \dot{T}_{zx}T_{zz} + \dot{T}_{zz}T_{zx} + \dot{T}_{yz}T_{yx}) \\
\dot{s}_z &= 2(-T_{xx}D - T_{xy}J + T_{yx}J - T_{yy}D) - \frac{\lambda}{2}(\dot{s}_x s_y - \dot{s}_y s_x + \dot{T}_{xx}T_{xy} - \dot{T}_{xy}T_{xx} \\
&\quad + \dot{T}_{yx}T_{yy} - \dot{T}_{yy}T_{yx} + \dot{T}_{zx}T_{zy} - \dot{T}_{zy}T_{zx}) \\
\dot{T}_{xx} &= 2(r_z D - T_{xy}B_z - T_{yx}B_z - s_z D) - \frac{\lambda}{2}(\dot{r}_y T_{zx} - \dot{r}_z T_{yx} + \dot{s}_y T_{xz} - \dot{s}_z T_{xy} - \\
&\quad \dot{T}_{zx}r_y + \dot{T}_{xy}s_z + \dot{T}_{yz}r_z - \dot{T}_{xz}s_y) - \gamma T_{xx} \\
\dot{T}_{xy} &= 2(-r_z J + s_z J + T_{xx}B_z - T_{yy}B_z) - \frac{\lambda}{2}(\dot{r}_y T_{zy} - \dot{r}_z T_{yy} + \dot{s}_x T_{xz} + \dot{s}_z T_{xx} \\
&\quad - \dot{T}_{xx}s_z + \dot{T}_{yy}r_z + \dot{T}_{xz}s_x - \dot{T}_{zy}r_y) - \gamma T_{xy}
\end{aligned}$$

$$\dot{T}_{xz} = 2(r_y J + s_x D - s_y J - T_{yz} B_z) - \frac{\lambda}{2}(\dot{r}_y T_{zz} - \dot{r}_z T_{yz} + \dot{s}_x T_{xy} - \dot{s}_y T_{xx} + \dot{T}_{xx} s_y - \dot{T}_{xy} s_x - \dot{T}_{zz} r_y + \dot{T}_{yz} r_z) - \gamma T_{xz}$$

$$\dot{T}_{yx} = 2(r_z J - s_z J + T_{xx} B_z - T_{yy} B_z) - \frac{\lambda}{2}(-\dot{r}_x T_{zx} + \dot{r}_z T_{xx} + \dot{s}_y T_{yz} - \dot{s}_z T_{yy} - \dot{T}_{xx} r_z + \dot{T}_{yy} s_z + \dot{T}_{zx} r_x - \dot{T}_{yz} s_y) - \gamma T_{yx}$$

$$\dot{T}_{yy} = 2(r_z D - s_z D + T_{xy} B_z + T_{yx} B_z) - \frac{\lambda}{2}(-\dot{r}_x T_{zy} + \dot{r}_z T_{xy} - \dot{s}_x T_{yz} - \dot{s}_z T_{yx} - \dot{T}_{xy} r_z - \dot{T}_{yx} s_z + \dot{T}_{yz} s_x + \dot{T}_{zy} r_x) - \gamma T_{yy}$$

$$\dot{T}_{yz} = 2(-r_x J + s_x J + s_y D + T_{xz} B_z) - \frac{\lambda}{2}(-\dot{r}_x T_{zz} + \dot{r}_z T_{xz} + \dot{s}_x T_{yy} - \dot{s}_y T_{yx} + \dot{T}_{yx} s_y - \dot{T}_{yy} s_x - \dot{T}_{xz} r_z + \dot{T}_{zz} r_x) - \gamma T_{yz}$$

$$\dot{T}_{zx} = 2(-r_x D - r_y J - T_{zy} B_z + s_y J) - \frac{\lambda}{2}(\dot{r}_x T_{yx} - \dot{r}_y T_{xz} + \dot{s}_y T_{zz} - \dot{s}_z T_{zy} + \dot{T}_{xx} r_y - \dot{T}_{yx} r_x - \dot{T}_{zz} s_y + \dot{T}_{zy} s_z) - \gamma T_{zx}$$

$$\dot{T}_{zy} = 2(r_x J - r_y D - s_x J + T_{zx} B_z) - \frac{\lambda}{2}(\dot{r}_x T_{yy} - \dot{r}_y T_{xy} - \dot{s}_x T_{zz} + \dot{s}_z T_{zx} + \dot{T}_{xy} r_y - \dot{T}_{yy} r_x - \dot{T}_{zx} s_z + \dot{T}_{zz} s_x) - \gamma T_{zy}$$

$$\dot{T}_{zz} = -\frac{\lambda}{2}(\dot{r}_x T_{yz} - \dot{r}_y T_{xz} + \dot{s}_x T_{zy} - \dot{s}_y T_{zx} + \dot{T}_{xz} r_y + \dot{T}_{zx} s_y - \dot{T}_{yz} r_x - \dot{T}_{zy} s_x)$$

4 Numerical Solutions

The equations of motion were solved numerically using *Mathematica*, based on the assumptions listed above and using the thermal equilibrium state as an initial condition. The function ParametricNDSolve was used to find the solutions, which can use many different methods for solving the system, but all work by "stepping" the system forward in increments the independent variable (in this case t). The step size and method used are completely adaptive, which gives it many advantages for tackling otherwise stiff systems [25].

4.1 Initial Conditions: Thermal States

For initial conditions, the qubits were assumed to be in the "X-type" thermal equilibrium states [26]. This also enables temperature to be included in the model as a parameter, and should allow a critical temperature [18] to be found, beyond which there is no entanglement. These states have the general form:

$$\varrho_T = \frac{1}{\mathcal{Z}} e^{-\frac{H}{kT}} = \begin{pmatrix} \rho_{11} & 0 & 0 & \rho_{14} \\ 0 & \rho_{22} & \rho_{23} & 0 \\ 0 & \rho_{32} & \rho_{33} & 0 \\ \rho_{41} & 0 & 0 & \rho_{44} \end{pmatrix}, \tag{17}$$

where T is the temperature, k is Boltzmann's constant and the non-zero matrix components are given by:

$$
\begin{aligned}
\rho_{11} &= \frac{1}{\mathcal{Z}} e^{-\frac{J}{2kT}} e^{-\frac{B_z}{kT}} \\
\rho_{44} &= \frac{1}{\mathcal{Z}} e^{-\frac{J}{2kT}} e^{\frac{B_z}{kT}} \\
\rho_{22} &= \frac{1}{\mathcal{Z}} e^{\frac{J}{2kT}} \cosh\left(\frac{\sqrt{J^2 + D^2}}{T}\right) \\
\rho_{33} &= \frac{1}{\mathcal{Z}} e^{\frac{J}{2kT}} \cosh\left(\frac{\sqrt{J^2 + D^2}}{T}\right) \\
\rho_{23} = \rho_{32}* &= -\frac{1}{\mathcal{Z}} e^{\frac{J}{2kT}} e^{-i\phi} \sinh\left(\frac{\sqrt{J^2 + D^2}}{T}\right),
\end{aligned}
$$

and where $\mathcal{Z}$ is the partition function, given by:

$$
\mathcal{Z} = \operatorname{Tr} e^{-\frac{H}{kT}} = 2\left(e^{-\frac{J}{2kT}} \cosh\left(\frac{B_z}{T}\right) + e^{\frac{J}{2kT}} \cosh\left(\frac{\sqrt{J^2 + D^2}}{T}\right)\right)
$$

where we also have:

$$
\tan\phi = \frac{D}{J}.
$$

This results in an initial thermal state where the Bloch vectors initially take a value in the z-component, but the others are zero. These values were obtained by converting the density matrix to the Bloch matrix and reading off the starting values [24].

Alongside temperature, the strengths of the Heisenberg exchange (J) and DM-interactions (D), the strength of the magnetic field (B_z), the damping constant (γ) and the coefficient for the non-linear term (λ) were all parameters in the model. Typical parameters [18, 8], $J = \pm 1$ (anti-ferromagnetic and ferromagnetic, respectively), $D = \frac{J}{10}$, $\lambda = 0.2$ and $\gamma = 0.2$ were chosen in the simulations.

4.2 Solutions for Bloch Vectors and the Correlation Matrix

The equations were solved with the initial conditions and parameter values above. For a range of kT from 0.1 to 10 and a field strength of $B_z = 0.5$ T, the Bloch vectors remained aligned in the z-direction, but with oscillating magnitudes that were increasingly damped as t approached 30 s.

4.2.1 General Form of the Solutions at $kT = 0.1$

Figure 1 shows the magnitude of the Bloch vectors for the duration of the evolution for both the ferromagnetic ($J = -1$, left) and anti-ferromagnetic ($J = 1$, right) cases. Both have an oscillating pattern, with the anti-ferromagnetic case tending towards zero as the system evolves and the ferromagnetic case tending towards -0.9929. As expected, the Bloch vectors take opposing signs throughout the evolution in the anti-ferromagnetic case. There is also an out-of-phase precession in the ferromagnetic case, which is a result of the anisotropic spin "canting" [11] from the DM interaction.

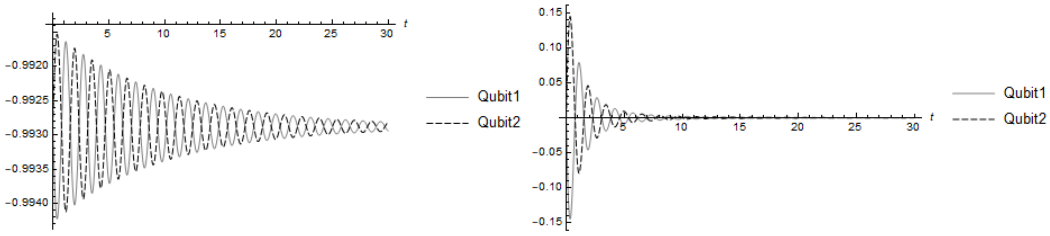

Figure 1: Evolution of Bloch vector z components for the ferromagnetic (left) and anti-ferromagnetic (right) cases.

The correlation matrix elements were also found throughout the evolution, with the T_{zx}, T_{xz}, T_{yz} and T_{zy} components being 0 throughout. Figure 2 shows the non-zero matrix components throughout the evolution for the anti-ferromagnetic case, and Figure 3 shows the ferromagnetic case.

The T_{xy} and T_{yx} components have the same absolute values throughout, but with opposing signs. T_{xx} and T_{yy} have matching curves, and T_{zz} has a consistent value of -1. As Figure 2 shows, all values aside from T_{zz} tend towards

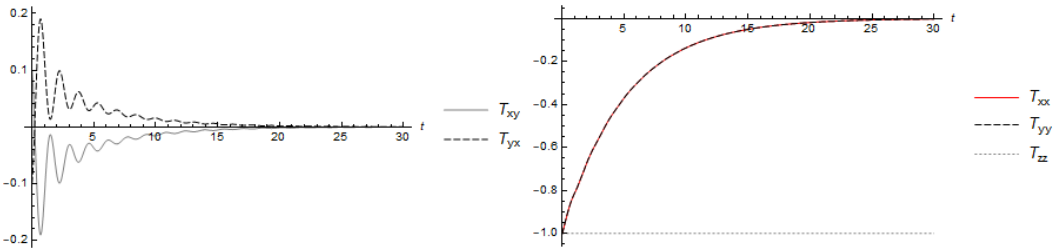

Figure 2: Non-zero matrix components in the anti-ferromagnetic case, with the T_{xy} and T_{yx} components on the left and the T_{xx}, T_{yy} and T_{zz} components on the right.

0 as the anti-ferromagnetic system evolves.

In the ferromagnetic case (Figure 3), the overall shape of the curves and their zero components are similar, except most of the magnitudes are smaller and the components are all flipped in sign. Only the T_{zz} component has the same magnitude as in the anti-ferromagnetic case.

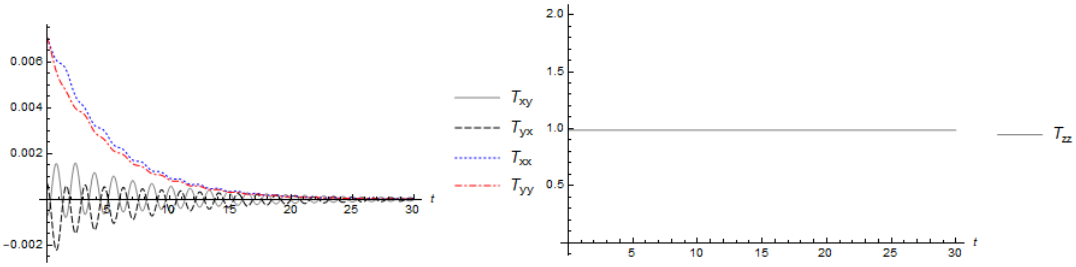

Figure 3: Non-zero matrix components in the ferromagnetic case, with the T_{zz} component on the right and the other non-zero components on the left.

4.2.2 Temperature Dependence of the Solutions

When the value of kT is increased, the evolution of the Bloch vectors takes the same overall shape, but with a reduced magnitude and range of oscillation. Figure 4 shows this for the ferromagnetic case and several values of kT, up to $kT = 10$.

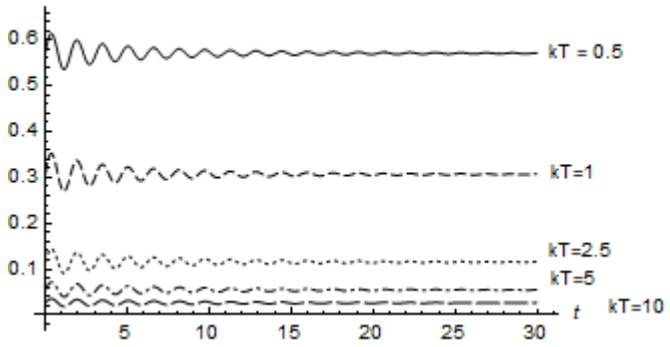

Figure 4: Absolute values for the z-component of a Bloch vector while kT is increased.

.

The variation in the correlation matrix elements follows the same pattern, with higher kT values corresponding to lower magnitudes of the matrix elements. This is shown in Figure 5 for the anti-ferromagnetic case and the T_{yx} component, with five illustrative values of kT displayed with a progressive offset.

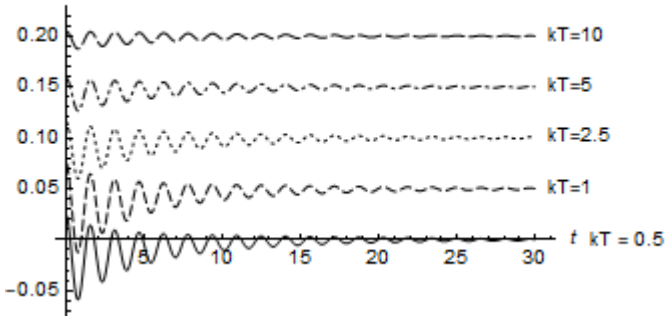

Figure 5: The variation in the T_{yx} matrix element as kT is increased from 0.5 to 10 J. These have been offset for clarity, in reality, all oscillations overlapped the $kT = 0.5$ line

The other matrix components behave in the same way, with some variation. For instance, the T_{zz} component remains a straight line but reduces in magnitude with increasing kT.

5 Non-Locality in the System

Non-locality in the system was calculated using the CHSH inequality [17], in the form used by Horst *et. al.* [22]. Given the Bell-CHSH operator $\mathcal{B}_{\text{CHSH}}$, which is defined:

$$\mathcal{B}_{\text{CHSH}} = \vec{a} \cdot \vec{\sigma} \otimes (\vec{b} + \vec{b}') \cdot \vec{\sigma} + \vec{a}' \cdot \vec{\sigma} \otimes (\vec{b} - \vec{b}') \cdot \vec{\sigma},$$

where $\vec{a}, \vec{a}', \vec{b}$ and $\vec{b}'$ are real-valued, three-dimensional unit vectors which are used to maximize the operator's expected value. With this in mind, the CHSH inequality can be written as:

$$|\operatorname{Tr}(\rho \mathcal{B}_{\text{CHSH}})| \leq 2.$$

Horodecki *et. al.* [21] showed that the maximum expected value of the Bell operator is given by:

$$\max_{\mathcal{B}_{\text{CHSH}}} \operatorname{Tr}(\rho \mathcal{B}_{\text{CHSH}}) = 2\sqrt{M(\rho)},$$

where

$$M(\rho) = \max_{j<k} \{h_j + h_k\}.$$

The h_j and h_k in this equation are the eigenvalues of the matrix $U = T^T T$, where T is the correlation matrix. In terms of M, the inequality is satisfied iff [27]:

$$M(\rho) \leq 1.$$

However, as Horst *et. al.* point out [22], using the function $B(\rho)$ makes the measure equal to the concurrence for two-qubit pure states. This function is defined:

$$B(\rho) = \sqrt{\max[0, M(\rho) - 1]}, \tag{18}$$

and gives $B(\rho) = 0$ if the state ρ doesn't violate the CHSH inequality. This form will be used in the analysis.

5.1 Non-Locality in Ferromagnetic and Anti-Ferromagnetic Cases

The dimer system considered violated the CHSH inequality in the anti-ferromagnetic but not the ferromagnetic case. For the anti-ferromagnetic case ($J > 0$), Figure 6 shows maximal violation at $t = 0$ s, for the initial singlet state, declining to a minimum value of 0.0023 at $t = 30$ s.

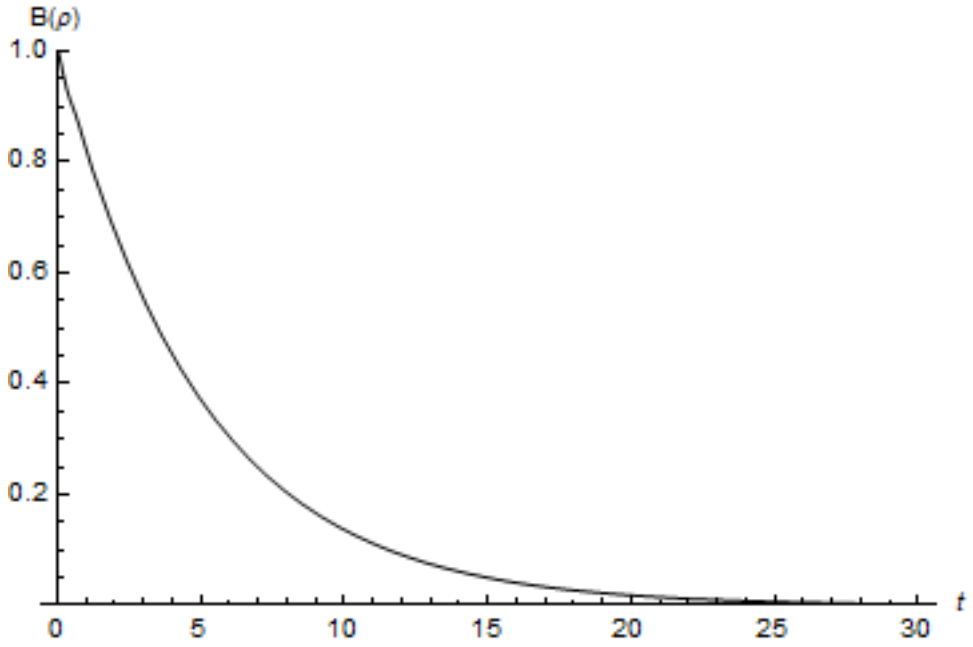

Figure 6: CHSH inequality violation for anti-ferromagnetic dimer at $kT = 0.1$

In contrast, there is no violation for the ferromagnetic case, with $B(\rho) = 0$ throughout.

5.2 The B_z and kT Dependence of Non-Locality

Non-locality in the system, as measured by $B(\rho)$, depends on both the magnetic field strength B_z and the temperature T, actually expressed with Boltzmann's constant as kT. Figure 7 shows the evolution of the system for a range of B and kT values.

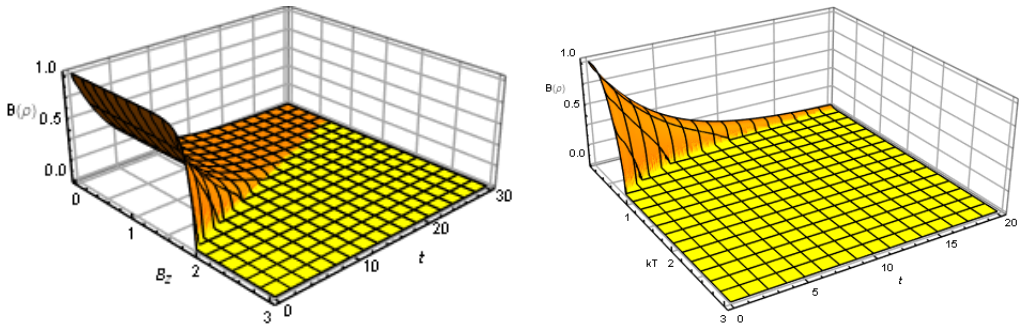

Figure 7: Values of $B(\rho)$ obtained for various values of magnetic field strength B_z (left) and temperature kT (right). Non-locality was detected in the orange region. Note that both parameters have "critical" values, beyond which there is no non-locality.

Figure 8 shows the values for $B(\rho)$ across a similar range of values, but shown as a snapshot at $t = 0$. This shows that non-locality is only observed for a small range of values of the parameters. After $kT = 0.9$ J and $B_z = 1.92$ T, the non-locality is lost. For the magnetic field, there is a sharp drop-off between the maximum of 1 (which remains the value even when $B_z = 1.5$ T) and the minimum at $B_z = 1.93$ T, while the change with temperature is a little more gradual.

In all cases of the ferromagnetic dimer, there is no non-locality for any values of B_z or kT. Additionally, while an analysis at a later time than $t = 0$ s would produce slightly different results, the overall pattern is the same and is best illustrated by the $t = 0$ s example.

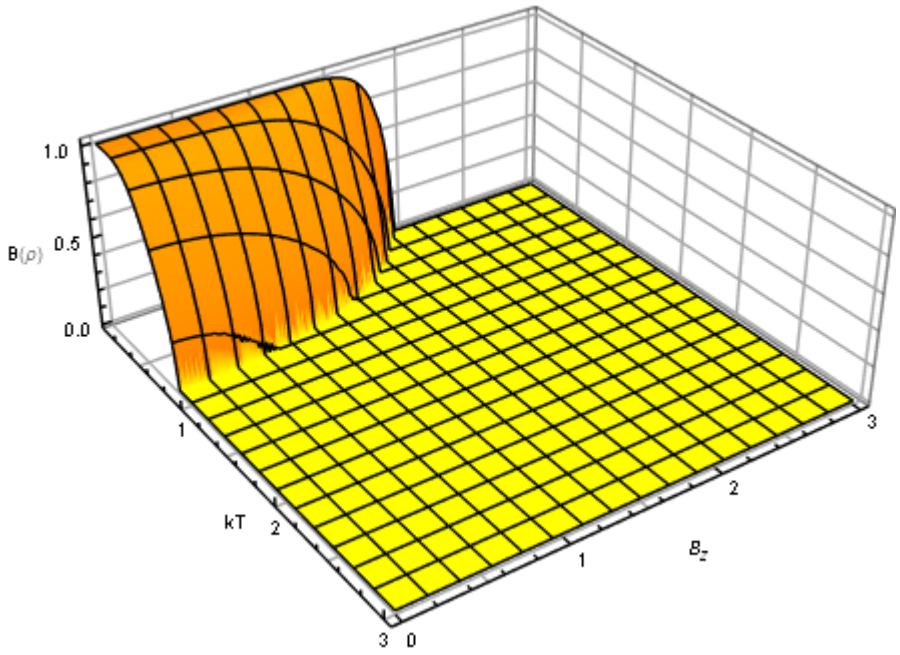

Figure 8: Values of $B(\rho)$ for different combinations of B_z and kT values, taken as a snapshot of the anti-ferromagnetic system at $t = 0$. Non-locality is detected in the orange region.

6 Relative Entropy of Entanglement Via Concurrence

Entanglement in the system was also calculated via concurrence [19]. The original form of the equation for concurrence comes from work defining the entanglement of formation $E(M)$ [28] for a mixed state M, with $E(M)$ being the minimum expected entanglement for any ensemble of pure states satisfying M. It has been found [19] that the entanglement of formation can be written as:

$$E(\psi) = \varepsilon(C(\psi)),$$

where C, the concurrence, is defined:

$$C(\psi) = \left| \left\langle \psi \middle| \tilde{\psi} \right\rangle \right|,$$

with $\tilde{\psi}$ being the spin-flipped version of ψ. Finally, ε is given by:

$$\varepsilon(C) = -\frac{1+\sqrt{1-C^2}}{2} \log_2 \frac{1+\sqrt{1-C^2}}{2} - \frac{1-\sqrt{1-C^2}}{2} \log_2 \frac{1-\sqrt{1-C^2}}{2}.$$

This function is monotonically increasing, going from 0 to 1 as C also goes from 0 to 1. This means that the concurrence itself can also been seen as a measure of entanglement, and it can be calculated directly from the density matrix for the system.

This approach was used for the analysis, so, in practice, concurrence was calculated using the eigenvalues of the Hermitian matrix R [19]:

$$R \equiv \sqrt{\sqrt{\rho}\tilde{\rho}\sqrt{\rho}}, \tag{19}$$

where the $\tilde{\rho}$ is the spin-flipped density matrix. This is calculated with:

$$\tilde{\rho} = (\sigma_y \otimes \sigma_y)\rho^*(\sigma_y \otimes \sigma_y), \tag{20}$$

where ρ^* is the complex conjugate of ρ. With this definition, and eigenvalues of this matrix indicated by λ_i, the concurrence can be written as:

$$C(\rho) = \max\{0, \lambda_1 - \lambda_2 - \lambda_3 - \lambda_4\}, \tag{21}$$

where the λ_1 is the numerically largest eigenvalue, λ_2 is the next largest and so on. This can also be calculated based on the square roots of the eigenvalues of the matrix $\rho\tilde{\rho}$. Each λ_i is a non-negative real number [19], and this was checked by analysis of any imaginary parts of the eigenvalues. In all cases, these were 0 or extremely small (of the order 10^{-15} or less), and so the formula is valid in this case.

6.1 Concurrence for Ferromagnetic and Anti-Ferromagnetic Cases

As with CHSH inequality violation, non-zero concurrence was obtained for the anti-ferromagnetic ($J = 1$) but not the ferromagnetic ($J = -1$) case. This is shown in Figure 9 for the anti-ferromagnetic case and the parameter values used before.

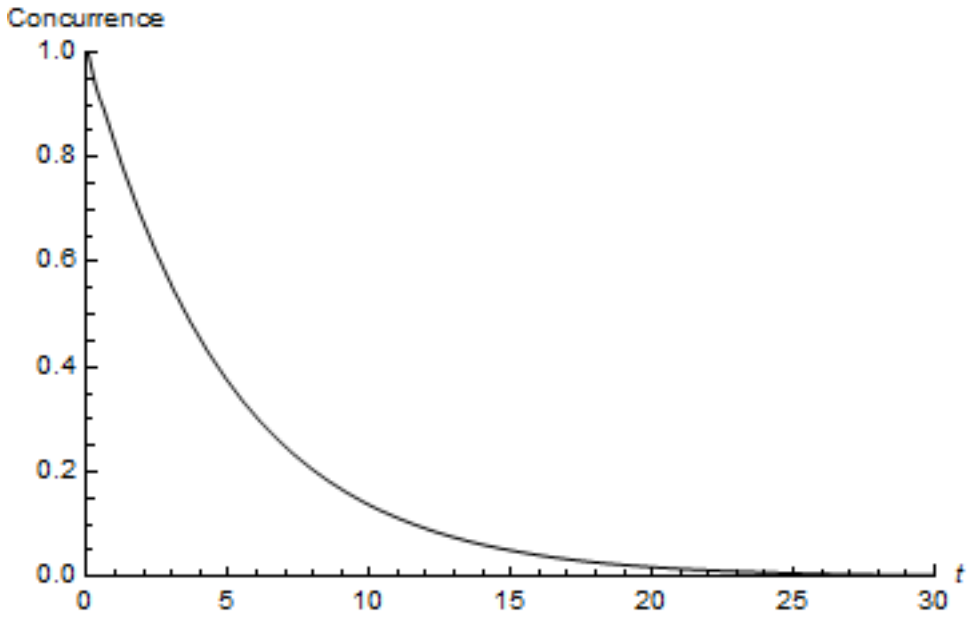

Figure 9: Concurrence in the anti-ferromagnetic dimer case considered, with $J = 1$.

The value for concurrence starts out at the maximum ($C = 1$) and then asymptotically declines to zero. However, throughout the entire evolution considered in this paper (up to $t = 50$ s) it always remained above zero in this case. In the ferromagnetic case ($J = -1$), it never reaches a value above zero and so there is no entanglement.

6.2 The B_z and kT Dependence of Concurrence

As for non-locality, the influence of kT and B_z values on concurrence was analyzed, both individually across the first 20 seconds of the dimer's evolution

and simultaneously as a snapshot at $t = 0$ s. Figure 10 shows the influence of kT and B_z on the entanglement in the system, from the initial state to 20 s into the evolution.

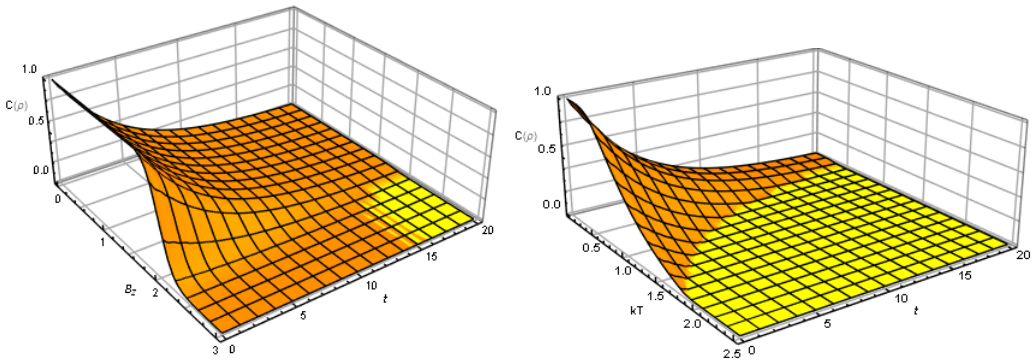

Figure 10: Variation in $C(\rho)$ throughout the dimer's evolution (up to $t = 20$ s) as B_z (left) and kT (right) are increased. Entanglement was detected in the orange region.

Note from Figure 7 and Figure 10 that there are values of kT (between 1 and 2 J) for which there is no non-locality but where there is entanglement as measured by concurrence. In contrast, non-locality is lost for values above $B_z = 2$ T and the degree of entanglement reduces substantially.

Figure 11 shows the variation in the initial value for concurrence with both kT and B simultaneously. As before, this analysis is performed at $t = 0$ s but the results retain their general form (albeit with smaller values) throughout the entanglement. Note that there is only entanglement initially if both B_z and kT fall within certain critical values.

Based on the numerical solutions, this gives a critical kT value of $kT_{crit} = 1.84$ J, where the J here is joules. For B_z, while the values decline substantially after $B_z = 2$ T, even at $B_z = 3.5$ T there is a small amount of detectable entanglement. However, we can establish $B_{z,crit} = 4$ T as the point where zero values begin to appear at minimum temperature. Beyond these values, the entanglement is lost.

Additionally, as shown by Figure 12, there are many values for B_z in which

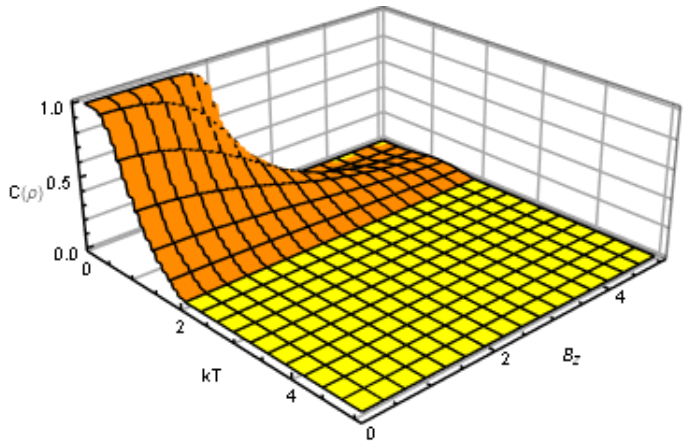

Figure 11: Values of $C(\rho)$ for the dimer system at $t = 0$ s as kT and B_z are increased.

increasing the temperature *increases* the entanglement, contrary to the results obtained in the rest of the analysis.

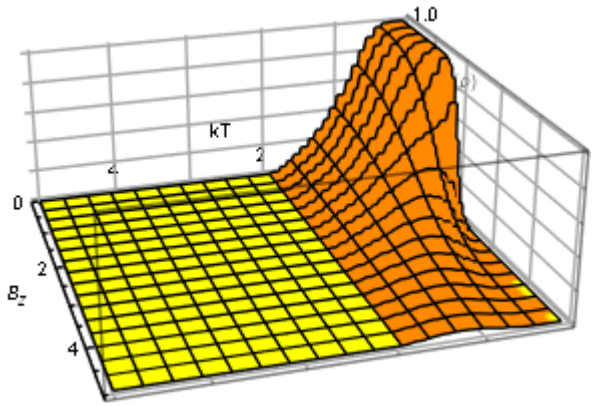

Figure 12: A rotated version of Figure 11, clearly showing values of B_z for which increasing kT also increases entanglement.

7 Discussion

Wieser's [7] non-linear master equation (Eq. (2)) was solved for a dimer system, with two important spin-spin interactions and open system effects included, across a range of values for both temperature and magnetic field. The results showed oscillations in the Bloch vectors, with initial peaks in the anti-ferromagnetic case up to ± 0.145, with progressively smaller values afterwards and quickly reaching zero. The five non-zero correlation matrix elements either took matching values with an opposite sign (T_{xy} and T_{yx}), the same value (T_{xx} and T_{yy} or remained constant like T_{zz}).

As expected from other results [18, 26], non-locality and entanglement were found in the anti-ferromagnetic but not the ferromagnetic case. Both non-locality and entanglement were detected early in the evolution and approached zero as it continued. In the case of non-locality (shown in Figures 6 and 7), this has been called "non-locality sudden death" [29] (in particular, in cases as discussed below where there is non-zero entanglement). Similarly, the loss of entanglement (Figures 9 and 10) has been called "finite time disentanglement" [30].

As identified by other authors [30], these effects are due to the parameter γ from the Lindblad term, and when local dephasing is switched off, the entanglement and non-locality remain with the same intensity throughout the evolution. However, this loss of entanglement will likely pose issues for quantum communications in the presence of similar open-system effects [31, 30].

Both non-locality and concurrence were also analyzed in the kT and B_z parameter space, in Figures 8, 11 and 12. At $B_z = 0$, the singlet state is the ground state of the system and the triplets are degenerate excited states. Increasing the temperature leads to the mixing of triplets with the singlets, decreasing the observed entanglement [18]. Likewise, increasing B_z splits the triplet states, making $|00\rangle$ the ground state, but then increasing the temperature brings in a singlet component and thereby increases entanglement, as shown clearly in Figure 12. Arnesen *et. al.* also detected this phenomenon [18], albeit at higher magnetic field values.

Figure 8 shows the CHSH inequality values in this parameter space. At the minimum temperature considered $kT = 0.1$ J, the non-locality is bro-

ken at a magnetic field strength of $B_{z,crit} = 1.92$ T, and at $B_z = 0$ T, the non-locality is broken when $kT_{crit} = 0.86$ J. For entanglement, the parameter space plot in Figure 11 shows a critical field strength value of $B_{z,crit} = 4$ T, measured at $kT = 0.1$ J, and a critical temperature of $kT_{crit} = 1.834$ J at $B_z = 0$ T.

Arnesen *et. al.* [18] studied the 1D Heisenberg model, producing a similar Hamiltonian to the one used here but without the DM-interaction included and with no open system effects. The authors found a critical temperature value of $kT_{crit} = \frac{J}{\ln(3)} \approx 0.91J$, where J here is the Heisenberg coupling constant. As in this report, Arnesen *et. al.* used a value of $J = 1$, so their values translate directly. For the magnetic field, in their case, they found a critical value of $B_{z,crit} = 4J$, again, expressed in the paper using the Heisenberg coupling and closely matching the results here.

Despite the agreement in terms of critical magnetic field, there are some important differences to note between this and other analyses [18, 26]. These analyses were conducted purely based on the Hamiltonian of the state, whereas the current analysis looks at the solutions to Wieser's quantum LLG equation [7], Eq. (2). However, the difference in the critical temperature is close to a perfect factor of 2, and is likely due to differences in the Hamiltonian.

Comparison of Figures 8 and 11 also shows that there are some parameter regions in the system for which there is entanglement without detectable non-locality through the basic CHSH measure. While the possibility of this is already well-known [32], in most cases the non-locality is simply "hidden" [33, 34] and is recoverable if a local filter is used prior to the Bell test. This analysis predicts the behaviour for a quantum LLG system between around $kT = 0.9$ J and 1.8 J, provided the magnetic field is weak enough to allow entanglement. There are some entangled states without this hidden non-locality [35], but it's likely that the simple test is the issue in this case.

The present analysis leaves much ground to explore. Firstly, the only spin-spin interactions considered were the Heisenberg exchange and the DM interaction. More interactions could easily be incorporated into a similar analysis, and a more realistic treatment should also include additional particles and non-nearest-neighbour interactions [18]. Future analyses could also incorporate other open system effects. Finally, the "lowest-order" version of Wieser's

equation (Eq. (2)) was solved here, while the version in Eq. (3) is likely more accurate.

Despite these limitations, this analysis has shown the form of a solution to Wieser's quantum LLG equation for a dimer system, incorporating important spin-spin interactions and open system effects, finding Bloch vectors and the system's correlation matrix. The CHSH inequality violations and concurrence values align with expectations from similar systems, but with some differences that likely stem from the more complicated model, the Hamiltonians used and the specific form of the solutions to the LLG equation.

References

[1] M. Lakshmanan, "The Fascinating World of the Landau-Lifshitz-Gilbert Equation: An Overview," *Philosophical Transactions: Mathematical, Physical and Engineering Sciences*, vol. 369, no. 1939, pp. 1280–1300, 2011.

[2] A. Hucht, S. Buschmann, and P. Entel, "Molecular Dynamics Simulations of the Dipolar-Induced Formation of Magnetic Nanochains and Nanorings," *Europhysics Letters (EPL)*, vol. 77, p. 57003, feb 2007.

[3] J. B. Bell, A. L. Garcia, and S. A. Williams, "Numerical Methods for the Stochastic Landau-Lifshitz Navier-Stokes Equations," *Phys. Rev. E*, vol. 76, p. 016708, Jul 2007.

[4] G. Boerner, J. Ehlers, and E. Rudolph, "Relativistic Spin Precession in Two-Body Systems.," *Astronomy and Astrophysics*, vol. 44, pp. 417–420, Nov. 1975.

[5] C. Chappert, A. Fert, and F. Van Dau, "The Emergence of Spin Electronics in Data Storage," *Nature Materials*, vol. 6, pp. 813 – 823, nov 2007.

[6] O. Eriksson, A. Bergman, L. Bergqvist, and J. Hellsvik, *Atomistic Spin Dynamics: Foundations and Applications*. Oxford University Press, 02 2017.

[7] R. Wieser, "Comparison of Quantum and Classical Relaxation in Spin Dynamics," *Phys. Rev. Lett.*, vol. 110, p. 147201, Apr 2013.

[8] R. Wieser, "Description of a Dissipative Quantum Spin Dynamics with a Landau-Lifshitz/Gilbert Like Damping and Complete Derivation of the Classical Landau-Lifshitz Equation," *The European Physical Journal B*, vol. 88, p. 77, Mar 2015.

[9] P. Mondal, A. Suresh, and B. K. Nikolić, "When Can Localized Spins Interacting with Conduction Electrons in Ferro- or Antiferromagnets be Described Classically via the Landau-Lifshitz Equation: Transition from Quantum Many-Body Entangled to Quantum-Classical Nonequilibrium States," *Phys. Rev. B*, vol. 104, p. 214401, Dec 2021.

[10] M. Mostafanejad, "Basics of the Spin Hamiltonian Formalism," *International Journal of Quantum Chemistry*, vol. 114, no. 22, pp. 1495–1512, 2014.

[11] V. E. Dmitrienko, E. N. Ovchinnikova, S. P. Collins, G. Nisbet, G. Beutier, Y. O. Kvashnin, V. V. Mazurenko, A. I. Lichtenstein, and M. I. Katsnelson, "Measuring the Dzyaloshinskii–Moriya Interaction in a Weak Ferromagnet," *Nature Physics*, vol. 10, no. 3, pp. 202 – 206, 2014.

[12] H.-B. Chen, P.-Y. Lo, C. Gneiting, J. Bae, Y.-N. Chen, and F. Nori, "Quantifying the Nonclassicality of Pure Dephasing," *Nature Communications*, vol. 10, no. 1, 2019.

[13] I. L. Chuang, R. Laflamme, P. W. Shor, and W. H. Zurek, "Quantum Computers, Factoring, and Decoherence," *Science*, vol. 270, no. 5242, pp. 1633–1635, 1995.

[14] E. Schrödinger, "Discussion of Probability Relations Between Separated Systems," *Mathematical Proceedings of the Cambridge Philosophical Society*, vol. 31, no. 4, p. 555–563, 1935.

[15] A. Einstein, B. Podolsky, and N. Rosen, "Can Quantum-Mechanical Description of Physical Reality Be Considered Complete?," *Phys. Rev.*, vol. 47, pp. 777–780, May 1935.

[16] J. S. Bell, "On the Einstein Podolsky Rosen Paradox," *Physics*, vol. 1, pp. 195–200, Nov 1964.

[17] J. F. Clauser, M. A. Horne, A. Shimony, and R. A. Holt, "Proposed Experiment to Test Local Hidden-Variable Theories," *Phys. Rev. Lett.*, vol. 23, pp. 880–884, Oct 1969.

[18] M. C. Arnesen, S. Bose, and V. Vedral, "Natural Thermal and Magnetic Entanglement in the 1D Heisenberg Model," *Phys. Rev. Lett.*, vol. 87, p. 017901, Jun 2001.

[19] W. K. Wootters, "Entanglement of Formation of an Arbitrary State of Two Qubits," *Phys. Rev. Lett.*, vol. 80, pp. 2245–2248, Mar 1998.

[20] S. Popescu and D. Rohrlich, "Thermodynamics and the Measure of Entanglement," *Physical Review A*, vol. 56, pp. R3319–R3321, nov 1997.

[21] R. Horodecki, P. Horodecki, and M. Horodecki, "Violating Bell Inequality by Mixed Spin-1/2 States: Necessary and Sufficient Condition," *Physics Letters A*, vol. 200, no. 5, pp. 340–344, 1995.

[22] B. Horst, K. Bartkiewicz, and A. Miranowicz, "Two-Qubit Mixed States More Entangled than Pure States: Comparison of the Relative Entropy of Entanglement for a Given Nonlocality," *Phys. Rev. A*, vol. 87, p. 042108, Apr 2013.

[23] G. Lindblad, "On the Generators of Quantum Dynamical Semigroups," *Communications in Mathematical Physics*, vol. 48, pp. 119–130, June 1969.

[24] O. Gamel, "Entangled Bloch Spheres: Bloch Matrix and Two-Qubit State Space," *Phys. Rev. A*, vol. 93, p. 062320, Jun 2016.

[25] Wolfram, " Numerical Operations on Functions," *Wolfram Documentation*.

[26] V. Azimi-Mousolou, A. Bergman, A. Delin, O. Eriksson, M. Pereiro, D. Thonig, and E. Sjöqvist, "Entanglement duality in spin-spin interactions," *Phys. Rev. A*, vol. 106, p. 032407, Sep 2022.

[27] R. Horodecki, "Two-Spin-1/2 Mixtures and Bell's Inequalities," *Physics Letters A*, vol. 210, no. 4, pp. 223–226, 1996.

[28] C. H. Bennett, D. P. DiVincenzo, J. A. Smolin, and W. K. Wootters, "Mixed-State Entanglement and Quantum Error Correction," *Phys. Rev. A*, vol. 54, pp. 3824–3851, Nov 1996.

[29] C. Bengtson, M. Stenrup, and E. Sjöqvist, "Quantum Nonlocality in the Excitation Energy Transfer in the Fenna-Matthews-Olson Complex," *International Journal of Quantum Chemistry*, vol. 116, no. 23, pp. 1763–1771, 2016.

[30] T. Yu and J. H. Eberly, "Finite-Time Disentanglement Via Spontaneous Emission," *Phys. Rev. Lett.*, vol. 93, p. 140404, Sep 2004.

[31] H. Aschauer and H. J. Briegel, *Quantum Communication and Decoherence*, pp. 235–261. Berlin, Heidelberg: Springer Berlin Heidelberg, 2002.

[32] R. F. Werner, "Quantum states with Einstein-Podolsky-Rosen Correlations Admitting a Hidden-Variable Model," *Phys. Rev. A*, vol. 40, pp. 4277–4281, Oct 1989.

[33] S. Popescu, "Bell's Inequalities and Density Matrices: Revealing "Hidden" Nonlocality," *Phys. Rev. Lett.*, vol. 74, pp. 2619–2622, Apr 1995.

[34] F. Hirsch, M. T. Quintino, J. Bowles, and N. Brunner, "Genuine Hidden Quantum Nonlocality," *Phys. Rev. Lett.*, vol. 111, p. 160402, Oct 2013.

[35] F. Hirsch, M. T. Quintino, J. Bowles, T. Vértesi, and N. Brunner, "Entanglement Without Hidden Nonlocality," *New Journal of Physics*, vol. 18, p. 113019, nov 2016.

8 Appendix: A More Detailed Derivation

While the whole derivation process was extensive (due to the large number of terms coming from the nested commutator in Eq. (4)), the vast majority of the process was applying the formulae from Section 3.1, particularly the commutators in Eqs. (12) and (17). For example, the following commutator comes from the $\vec{r} \cdot \vec{\sigma}_1 \otimes \hat{1}$ term in the two-qubit parametrization (Eq. (7)) and the B_z term in the Hamiltonian (Eq. (6)):

$$\text{Term 1} = [(r_x\sigma_x + r_y\sigma_y + r_z\sigma_z) \otimes \hat{1}, B_z(\sigma_z \otimes \hat{1} + \hat{1} \otimes \sigma_z)] \tag{22}$$

First, note that only the first B_z term in Eq. (24) has a non-zero commutator, because of the relation in Eq. (14). For the second term, we can also use Eq. (14) to write:

$$\text{Term 1} = B_z(r_x[\sigma_x, \sigma_z] + r_y[\sigma_y, \sigma_z] + r_z[\sigma_z, \sigma_z]) \otimes \hat{1},$$

where we can pull B_z and r_i out of the commutators because they are scalars. Then, using Eq. (12), we find:

$$\text{Term 1} = 2iB_z(-r_x\sigma_y + r_y\sigma_x) \otimes \hat{1},$$

which can be expressed more neatly if we define $r_{ij} = r_i\sigma_j - r_j\sigma_i$ for $i, j \in x, y, z$, and write:

$$\text{Term 1} = -2iB_z r_{xy} \otimes \hat{1}.$$

Another example term, from the same $\vec{r} \cdot \vec{\sigma}_1 \otimes \hat{1}$ term hitting the $J\sigma_x \otimes \sigma_x$ term, shows the use of Eq. (17) in the derivation. We can write:

$$\text{Term 2} = [(r_x D_{x0} + r_y D_{y0} + r_z D_{z0}, JD_{xx}],$$

where we've used the Dirac matrices to express the commutator, and again we can remove r_i and J from the commutators because they are scalars. This leads to:

$$\begin{aligned}\text{Term 2} &= r_x[D_{x0}, D_{xx}] + r_y[D_{y0}, D_{xx}] + r_z[D_{z0}, D_{xx}] \\ &= 2ir_y(\theta_{yx\mu}\epsilon_{0x\nu} + \epsilon_{yx\mu}\theta_{0x\nu})D_{\mu\nu} + 2ir_z(\theta_{zx\delta}\epsilon_{0x\rho} + \epsilon_{zx\delta}\theta_{0x\rho})D_{\delta\rho} \\ &= 2i(-r_y D_{zx} + r_z D_{yx}),\end{aligned}$$

where the third line follows from the second based on the rule in Eq. (18), with the first θ term for both r_y and r_z having two non-matching indices. The majority of terms were calculated in this way, including the nested commutator terms. This filled out the right hand side of Eq. (4).

The left hand side of Eq. (4) was calculated using the Bloch vector parametrization in Eq. (7). Explicitly, this was:

$$\dot{\varrho} = \frac{1}{4}(\dot{\vec{r}} \cdot \vec{\sigma}_1 \otimes \hat{1} + \hat{1} \otimes \dot{\vec{s}} \cdot \vec{\sigma}_2 + \dot{T}_{kl}\sigma_{1,k} \otimes \sigma_{2,l}).$$

From here, as described in Section 3.2, the terms were arranged as coefficients of the Dirac matrices, and the equations of motion were formed by matching coefficients on each side. This led to the equations of motion that were solved in this paper, coming from Eq. (4) and ultimately from Wieser's [7] version (Eq. (2)). The full equations of motion are reproduced below, with the explicit t dependence of the r_i, s_i and T_{ij} omitted on the right-hand side for clarity:

$$\begin{aligned}\dot{r}_x(t) = {} & 2(\gamma r_x + J(T_{zy} - T_{yz}) - DT_{zx} - B_z r_y) + \lambda(B_z(r_x r_z + T_{xx}T_{zx} - 2T_{yy}T_{zx} + \\ & T_{xy}T_{zy} + 2T_{yx}T_{zy} + T_{xz}T_{zz}) + J(r_y T_{xy} + r_z T_{xz} - 2r_y T_{yx} + s_y T_{yx} + r_x T_{yy} - s_x T_{yy} - \\ & 2r_z T_{zx} + s_z T_{zx} + r_x T_{zz} - s_x T_{zz}) + D(-r_y T_{xx} - r_x T_{yx} - 2r_y T_{yy} - 2r_z T_{zy} + s_z T_{zy} - \\ & s_y T_{zz}))\end{aligned}$$

$$\begin{aligned}\dot{r}_y(t) = {} & 2(-\gamma r_y + J(T_{xz} - T_{zx}) - DT_{zy} + B_z r_x) + \lambda(B_z(r_y r_z + T_{xx}T_{zx} + 2T_{xy}T_{zx} - \\ & 2T_{xx}T_{zy} + T_{yy}T_{zy} + T_{yz}T_{zz}) + J(r_y T_{xx} - s_y T_{xx} - 2r_x T_{xy} + s_x T_{xy} + r_x T_{yx} + r_z T_{yz} - \\ & 2r_z T_{zy} + s_z T_{zy} + r_y T_{zz} - s_y T_{zz}) + D(2r_x T_{xx} + r_y T_{xy} + r_x T_{yy} + 2r_z T_{zx} - s_z T_{zx} + \\ & s_x T_{zz}))\end{aligned}$$

$$\begin{aligned}\dot{r}_z(t) = {} & 2(D(T_{xx} + T_{yy}) + J(-T_{xy} + T_{yx})) + \lambda(B_z(-r_x^2 - r_y^2 - T_{xx}^2 - T_{xy}^2 - \\ & T_{xz}^2 - T_{xx}T_{yx} - 2T_{xy}T_{yx} + 2T_{xx}T_{yy} - T_{yy}^2 - T_{yz}^2) + J(r_z T_{xx} - s_z T_{xx} - 2r_x T_{xz} + \\ & s_x T_{xz} + r_z T_{yy} - s_z T_{yy} - 2r_y T_{yz} + s_y T_{yz} + r_x T_{zx} + r_y T_{zy}) + D(r_z T_{xy} - s_z T_{xy} + \\ & s_y T_{xz} - r_z T_{yx} + s_z T_{yx} - s_x T_{yz} - r_y T_{zx} + r_x T_{zy}))\end{aligned}$$

$\dot{s}_x(t) = 2(-\gamma s_x + DT_{xz} + J(T_{yz} - T_{zy}) - B_z s_y) + \lambda(B_z(s_x s_z + T_{xx}T_{xz} - 2T_{xz}T_{yy} + 2T_{xy}T_{yz} + T_{yx}T_{yz} + T_{zx}T_{zz}) + J(r_y T_{xy} - 2s_y T_{xy} + r_z T_{xz} - 2s_z T_{xz} + s_y T_{yx} - r_x T_{yy} + s_x T_{yy} + s_z T_{zx} - r_x T_{zz} + s_x T_{zz}) + D(s_y T_{xx} + s_x T_{xy} + 2s_y T_{yy} - r_z T_{yz} + 2s_z T_{yz} + r_y T_{zz}))$

$\dot{s}_y(t) = 2(-\gamma s_y + DT_{yz} + J(-T_{xz} + T_{zx}) + B_z s_x) + \lambda(B_z(s_y s_z + T_{xx}T_{xz} + T_{xy}T_{xz} + T_{xz}T_{yx} + -2T_{xx}T_{yz} + T_{yy}T_{yz} + T_{zy}T_{zz}) + J(-r_y T_{xx} + s_y T_{xx} + s_x T_{xy} + r_x T_{yx} - 2s_x T_{yx} + r_z T_{yz} - 2s_z T_{yz} + s_z T_{zy} - r_y T_{zz} + s_y T_{zz}) + D(-2s_x T_{xx} + r_z T_{xz} - 2s_z T_{xz} - s_y T_{yx} - s_x T_{yy} - r_x T_{zz}))$

$\dot{s}_z(t) = 2(D(-T_{xx} - T_{yy}) + J(T_{xy} - T_{yx})) + \lambda(B_z(-s_x^2 - s_y^2 - T_{xx}^2 - T_{xx}T_{xy} - T_{xy}^2 - T_{xy}T_{yx} - T_{yx}^2 + 2T_{xx}T_{yy} - T_{yy}^2 - T_{zx}^2 - T_{zy}^2) + J(-r_z T_{xx} + s_z T_{xx} + s_x T_{xz} - r_z T_{yy} + s_z T_{yy} + s_y T_{yz} + r_x T_{zx} - 2s_x T_{zx} + r_y T_{zy} - 2s_y T_{zy}) + D(-r_z T_{xy} + s_z T_{xy} + s_y T_{xz} + r_z T_{yx} - s_z T_{yx} - s_x T_{yz} - r_y T_{zx} + r_x T_{zy}))$

$\dot{T}_{xx}(t) = 2(B_z(-T_{xy} - T_{yx}) + D(-r_z + s_z)) + \lambda(B_z(r_z T_{xx} + s_z T_{xx} + s_x T_{xz} - r_z T_{yy} - s_z T_{yy} + s_y T_{yz} + r_x T_{zx} + r_y T_{zy}) + J(-r_y^2 - r_z^2 + 2r_y s_y - s_y^2 + 2r_z s_z - s_z^2 - T_{xy}^2 - T_{xz}^2 + 2T_{xy}T_{yx} - T_{yx}^2 + 2T_{xz}T_{zx} - T_{zx}^2) + D(-r_x r_y + s_x s_y + T_{xx}T_{xy} - T_{xx}T_{yx} + T_{xy}T_{yy} - T_{yx}T_{yy} + T_{xz}T_{yz} - T_{zx}T_{zy})) - \gamma T_{xx}$

$\dot{T}_{xy}(t) = 2(B_z(T_{xx} - T_{yy}) + J(r_z - s_z)) + \lambda(B_z(s_z T_{xx} + r_z T_{xy} + s_z T_{xy} + s_y T_{xz} + r_z T_{yx} - s_x T_{yz} - r_y T_{zx} + r_x T_{zy}) + J(r_x r_y - 2r_y s_x + s_x s_y + T_{xx}T_{xy} - T_{xx}T_{yx} + T_{xy}T_{yy} - T_{yx}T_{yy} - T_{xz}T_{yz} + 2T_{xz}T_{zy} - T_{zx}T_{zy}) + D(-r_y^2 - r_z^2 - s_x^2 + 2r_z s_z - s_z^2 - T_{xx}^2 - T_{xz}^2 - 2T_{xx}T_{yy} - T_{yy}^2 - T_{zy}^2)) - \gamma T_{xy}$

$\dot{T}_{xz}(t) = 2(-B_z T_{yz} + J(-r_y + s_y) - Ds_x) + \lambda(B_z(-2s_x T_{xx} - s_y T_{xx} - 2s_y T_{xy} + r_z T_{xz} + s_x T_{yy} + r_x T_{zz}) + J(r_x r_z - 2r_z s_x + s_x s_z + T_{xx}T_{xz} + 2T_{xy}T_{yz} - T_{yx}T_{yz} - T_{xx}T_{zx} - T_{xy}T_{zy} + T_{xz}T_{zz} - T_{zx}T_{zz}) + D(-2r_z s_y + s_y s_z + T_{xy}T_{xz} - 2T_{xx}T_{yz} - T_{yy}T_{yz} - T_{zy}T_{zz})) - \frac{1}{2}\gamma T_{xz}$

$\dot{T}_{yx}(t) = 2(B_z(T_{xx} - T_{yy}) + J(-r_z + s_z) + \lambda(B_z(r_z T_{xx} + r_z T_{xy} + s_z T_{xy} - s_y T_{xz} + s_z T_{yx} + s_x T_{yz} + r_y T_{zx} - r_x T_{zy}) + J(r_x r_y - 2r_x s_y + s_x s_y - T_{xx}T_{xy} + T_{xx}T_{yx} - T_{xy}T_{yy} + T_{yx}T_{yy} - T_{xz}T_{yz} + 2T_{yz}T_{zx} - T_{zx}T_{zy}) + D(r_x^2 + r_z^2 + s_y^2 - 2r_z s_z + s_z^2 + T_{xx}^2 + 2T_{xx}T_{yy} + T_{yy}^2 + T_{yz}^2 + T_{zx}^2)) - \gamma T_{yx}$

$\dot{T}_{yy}(t) = 2(B_z(T_{xy} + T_{yx}) + D(-r_z + s_z)) + \lambda(B_z(-r_z T_{xx} - s_z T_{xx} + s_x T_{xz} + r_z T_{yy} + s_z T_{yy} + s_y T_{yz} + r_x T_{zx} + r_y T_{zy}) + J(-r_x^2 - r_z^2 + 2r_x s_x - s_x^2 + 2r_z s_z - s_z^2 - T_{xy}^2 + 2T_{xy}T_{yx} - T_{yx}^2 - T_{yz}^2 + 2T_{yz}T_{zy} - T_{zy}^2) + D(r_x r_y - s_x s_y + T_{xx}T_{xy} -$

$T_{xx}T_{yx} + T_{xy}T_{yy} - T_{yx}T_{yy} - T_{xz}T_{yz} + T_{zx}T_{zy})) - \gamma T_{yy}$

$\dot{T}_{yz}(t) = 2(B_z T_{xz} - Ds_y + J(r_x - s_x)) + \lambda(B_z(T_{yx} - 2s_y T_{yy} + r_z T_{yz} + r_y T_{zz}) + J(r_y r_z - 2r_z s_y + s_y s_z - T_{xy}T_{xz} + 2T_{xz}T_{yx} + T_{yy}T_{yz} - T_{yx}T_{zx} - T_{yy}T_{zy} + T_{yz}T_{zz} - T_{zy}T_{zz}) + D(2r_z s_x - s_x s_z + T_{xx}T_{xz} + 2T_{xz}T_{yy} - T_{yx}T_{yz} + T_{zx}T_{zz})) - \frac{1}{2}\gamma T_{yz}$

$\dot{T}_{zx}(t) = 2(-B_z T_{zy} + Dr_x + J(r_y - s_y)) + \lambda(B_z(-2r_x T_{xx} - r_y T_{xx} - r_y T_{xy} - r_y T_{yx} + r_x T_{yy} + s_z T_{zx} + s_x T_{zz}) + J(r_x r_z - 2r_x s_z + s_x s_z - T_{xx}T_{xz} - T_{yx}T_{yz} + T_{xx}T_{zx} - T_{xy}T_{zy} + 2T_{yx}T_{zy} - T_{xz}T_{zz} + T_{zx}T_{zz}) + D(-r_y r_z + 2r_y s_z - T_{yx}T_{zx} + 2T_{xx}T_{zy} + T_{yy}T_{zy} + T_{yz}T_{zz})) - \frac{1}{2}\gamma T_{zx}$

$\dot{T}_{zy}(t) = 2(B_Z T_{zx} + Dr_y + J(-2r_x + 2s_x)) + \lambda(B_z(r_y T_{xx} - 2r_x T_{xy} - r_x T_{yx} - 2r_y T_{yy} + s_z T_{zy} + s_y T_{zz}) + J(r_y r_z - 2r_y s_z + s_y s_z - T_{xy}T_{xz} - T_{yy}T_{yz} + 2T_{xy}T_{zx} - T_{yx}T_{zx} + T_{yy}T_{zy} - T_{yz}T_{zz} + T_{zy}T_{zz}) + D(r_x r_z - 2r_x s_z - T_{xx}T_{zx} - 2T_{yy}T_{zx} + T_{xy}T_{zy} - T_{xz}T_{zz})) - \frac{1}{2}\gamma T_{zy}$

$\dot{T}_{zz}(t) = \lambda(B_z(-2r_x T_{xz} - 2r_y T_{yz} - 2s_x T_{zx} - 2s_y T_{zy}) + J(-r_x^2 - r_y^2 + 2r_x s_x - s_x^2 + 2r_y s_y - s_y^2 - T_{xz}^2 - T_{yz}^2 + 2T_{xz}T_{zx} - T_{zx}^2 + 2T_{yz}T_{zy} - T_{zy}^2) + D(-2r_y s_x + 2r_x s_y 2T_{yz}T_{zx} + 2T_{xz}T_{zy}))$